A Quantum Chemical Study of the Type IV Nucleophilic Substitution Reaction and Dissociation of the β-Nicotinamide Glycosyl Bond in the Gas Phase Using Semiempirical PM3 Calculations

Stefan Schröder,† Neil Buckley, Norman J. Oppenheimer,* and Peter A. Kollman*

Contribution from the Department of Pharmaceutical Chemistry, School of Pharmacy, S-926, Box 0446, The University of California, San Francisco, California 94143.
Received January 23, 1992

Abstract: The type IV nucleophilic substitution reaction at the anomeric carbon of β-nicotinamide riboside$^+$ was studied in the gas phase using the semiempirical PM3 method. Because there are few computational studies of displacement reactions on a positively charged substrate, the isoenergetic displacements of dimethyl ether on the trimethyloxonium cation and trimethylamine on the tetramethylammonium cation were studied to provide base line comparisons. The results are compared to the thermodynamics of the unimolecular dissociation reaction and to prototype reactions of the extensively studied S_N2(type I) reaction. The experimentally determined dissociative character of the hydrolysis of β-nicotinamide riboside$^+$ can be rationalized in terms of the gas-phase calculations; the results suggest that the nitrogen–carbon bond must be broken almost entirely before either external nucleophile or solvent can react with the oxocarbenium ion intermediate. The structures for the inversion and retention reactions are different, in contrast to a suggestion made by Sinnott and Jencks (Sinnott, M. L.; Jencks, W. P. *J. Am. Chem. Soc.* **1980**, *102*, 2026–2032) that inversion and retention should proceed through a single activated complex. General differences between nucleophilic displacement reactions on neutral and positively charged substrates are discussed.

The nicotinamide–ribosyl bond of β-nicotinamide adenine dinucleotide (NAD^+) is hydrolytically unstable. Hydrolysis is pH independent below pH 7 and is accelerated by a factor of 10^4 at alkaline pH; above pH 13, hydrolysis is again pH independent. Cleavage of the nicotinamide bond is catalyzed by a series of enzymes including polyADP-ribose synthetase, cyclic ADPribose synthase, various ADP(ribose) transferases (both endogenous proteins and toxins), and NAD-glycohydrolases.[1-4] The mechanisms for the chemical and enzymatic cleavage of the nicotinamide–glycosyl bond have not been fully characterized.

The overall reaction is a type III/IV nucleophilic substitution in which the positively charged pyridinium leaving group (LG) is replaced with a negatively charged nucleophile (type III) or neutral nucleophile or solvent molecule (type IV).[5] Type IV reactions at saturated carbon have been studied extensively in chlorobenzene solvent with piperidine as the nucleophile by Katritzky and co-workers, who used highly arylated pyridines as leaving groups.[6,7] They concluded that tertiary alkyl substrates invariably solvolyze by a unimolecular mechanism, whereas secondary and primary alkyl substrates can undergo both uni- and bimolecular reactions, with the S_N2 process effectively competing in more nucleophilic solvents.

Substitutions of various neutral and positively charged leaving groups at the anomeric carbon of furanosides and pyranosides are commonly believed to be S_N1 reactions that proceed with the formation of an intermediate oxocarbenium ion. The rates of specific-acid-catalyzed hydrolysis of 2-substituted methyl glucopyranosides (LG = $HOMe^+$) follow the Taft linear free energy relation (LFER) with a large negative ρ^* consistent with a dissociative mechanism.[8] Handlon and Oppenheimer[9] have recently shown that the pH-independent hydrolyses of a series of 2′-substituted nicotinamide arabinosides (LG = nicotinamide$^+$) follow the Taft LFER with ρ_I values of −6.7. Measurements of kinetic α secondary deuterium isotope effects in the nonenzymatic cleavage of the glycosyl bond of NAD^+ indicate a significant amount of sp^2 hybridization at the anomeric carbon at the transition state for both the chemical and enzyme-catalyzed reactions.[10,11] Johnson et al.,[12] observed specific-base-catalyzed cleavage of the nicotinamide–ribosyl bond that is clearly the result of diol ionization and not the result of direct nucleophilic participation of hydroxide. The mechanism(s) by which enzymes catalyze cleavage of the nicotinamide–ribosyl bond remains obscure.

The presence of a solvent-equilibrated glycosyl oxocarbenium ion intermediate in the solvolysis of glycosides has been challenged by Jencks and co-workers. Young and Jencks[13a] originally estimated the lifetime of the glycopyranosyl oxocarbenium ion intermediate to be less than 10^{-15} s, and therefore the species could not become solvent equilibrated; indeed, because for this species there would be no barrier to collapse to products, it would not appear on a reaction coordinate diagram and therefore would not be a true intermediate.[14] Recently, Amyes and Jencks[13b] reevaluated the original data of Young and Jencks,[13a] and they now estimate the lifetime for glycosyl oxocarbenium ions to be on the order of 10^{-12} s, which is still too short to allow solvent equilibration. They concluded that such short lifetimes would require some degree of nucleophilic participation in the activated complex to stabilize the incipient oxocarbenium species. Sinnott and Jencks[15] presented stereochemical and solvent selectivity evidence

* Author to whom correspondence should be addressed.
† Present address: Schering AG, PCH/TCH, D-1000 Berlin 65, Germany.

(1) Moss, J.; Vaughan, M. *Annu. Rev. Biochem.* **1979**, *48*, 581–600.
(2) Ueda, K.; Hayaishi, O. *Annu. Rev. Biochem.* **1985**, *54*, 73–100.
(3) Hayaishi, O., Ueda, K., Eds. *ADP-Ribosylation Reactions: Biology and Medicine*; Academic Press: New York, 1982.
(4) Price, S. R.; Pekala, P. H. In *Pyridine Nucleotide Coenzymes: Chemical, Biochemical and Medical Aspects*; Dolphin, D., Poulson, R., Avramovic, O., Eds.; J. Wiley and Sons, Inc.: New York, 1987; Vol. 2B, pp 513–548.
(5) The Hughes–Ingold terminology for classification of nucleophilic reactions will be used here; thus, the reactions of neutral substrates—alkyl chlorides, tosylates, etc.—with negative or neutral nucleophiles are types I and II, respectively, while the reactions of positive substrates—pyridiniums, sulfoniums, oxoniums, etc.—with negative or neutral nucleophiles are types III and IV, respectively. Ingold, C. K. *Structure and Mechanism in Organic Chemistry*; Cornell University Press: Ithaca, NY, 1953; p 346.
(6) Katritzky, A. R.; Brycki, B. E. *J. Phys. Org. Chem.* **1988**, *1*, 1–20.
(7) Katritzky, A. R.; Musumarra, G. *Chem. Soc. Rev.* **1984**, *13*, 47–68.
(8) Marshall, R. D. *Nature* **1963**, *199*, 998–999.
(9) Handlon, A.; Oppenheimer, N. J. *J. Org. Chem.* **1991**, *56*, 5009–5010.
(10) Bull, H. G.; Ferraz, J. P.; Cordes, E. H.; Ribbi, A.; Apitz-Castro, R. *J. Biol. Chem.* **1978**, *253*, 5186–5192.
(11) Ferraz, J. P.; Bull, H. G.; Cordes, E. H. *Arch. Biochem. Biophys.* **1978**, *191*, 431–436.
(12) Johnson, R. W.; Marschner, T. M.; Oppenheimer, N. J. *J. Am. Chem. Soc.* **1988**, *110*, 2257–2263.
(13) (a) Young, P. R.; Jencks, W. P. *J. Am. Chem. Soc.* **1977**, *99*, 8238–8248. (b) Amyes, T. L.; Jencks, W. P. *J. Am. Chem. Soc.* **1989**, *111*, 7888–7900.
(14) Jencks, W. P. *Acc. Chem. Res.* **1980**, *13*, 161–169.
(15) Sinnott, M. L.; Jencks, W. P. *J. Am. Chem. Soc.* **1980**, *102*, 2026–2032.

0002-7863/92/1514-8232$03.00/0

Table I. Calculated Energies[a] for Dissociation in the Gas Phase

substrate	ΔH_f	cation	ΔH_f	leaving group	ΔH_f	ΔH_R
$(CH_3)_3O^+$	161.0	CH_3^+	256.5	$(CH_3)_2O$	-48.3	47.2
$(CH_3)_4N^+$	149.4	CH_3^+	256.5	$(CH_3)_3N$	-10.9	96.2
CH_3NA^+[b]	148.3	CH_3^+	256.5	NA	-8.8	99.4
$CH_3OCH_2O(CH_3)_2^+$[c,d]	116.1	$CH_3OCH_2^+$	165.1	$(CH_3)_2O$	-48.3	0.7
$CH_3OCH_2N(CH_3)_3^+$	113.5	$CH_3OCH_2^+$	165.1	$(CH_3)_3N$	-10.9	40.7
$CH_3OCH_2NA^+$[b]	110.4	$CH_3OCH_2^+$	165.1	NA	-8.8	45.9
β-NR^+[b,e]	-23.3	riboside$^+$	26.0	NA	-8.8	40.5

[a] All energies are reported in kcal/mol. [b] Abbreviations used: NA = nicotinamide, NR = β-nicotinamide riboside. [c] The (methoxymethyl)dimethyloxonium cation dissociates without a barrier; therefore, the C-O bond was constrained in the reported structure. [d] The O2′-β-NR-diolate cation cleaves the C1′-C2′ bond without a barrier; therefore, this bond was constrained in the reported structure. [e] The O2′-riboside structure corresponds to the 1,2-anhydro sugar proposed for anchimeric assistance.

for the participation of the incoming nucleophile and the leaving group in the transition state for the solvolysis of β- and α-1-fluoroglucose in ethanol–trifluoroethanol mixtures. These results were rationalized in terms of an "exploded" transition state[16] in which the incipient oxocarbenium species is stabilized electrostatically by both the entering and leaving groups.

In an attempt to understand this chemistry, we have investigated the hydrolysis of β-nicotinamide riboside$^+$ in the gas phase with the semiempirical PM3 method. Theoretical approaches to the mechanism of nucleophilic substitution reactions have concentrated almost exclusively on the S_N2(type I) reaction (see refs 17 and 18 for two recent examples). Because the gas-phase and solution rate constants for these reactions typically differ by 20 orders of magnitude, the nucleophilic attack of chloride on CH_3Cl has become the prototype case in efforts to include solvent effects in theoretical calculations.[19-24] In contrast, we found only one series of papers from Ford's group[25-27] in which the nucleophilic displacement of a neutral leaving group (N_2) from a positively charged substrate (RN_2^+) was studied. Therefore, we began our investigation with two simple model systems for the type IV nucleophilic substitution reaction: the isoenergetic attacks of dimethyl ether on the trimethyloxonium cation (Meerwein salt) and of trimethylamine on the tetramethylammonium cation. For comparison, the gas-phase dissociative reactions for the substrates were also calculated. With the insight gained from these reactions, we then studied the gas-phase reactions for chloride displacement on β-chlororibose (type I) and water on β-nicotinamide riboside$^+$ (type IV).

Methods

All calculations were carried out by using the recently described PM3 semiempirical molecular orbital procedure[28] as implemented in the MOPAC 5.0 program package.[29] The choice of this method instead of the AM1 methodology[30] was based on our previous results for hydrogen-bonding energies and geometries.[31] With a few exceptions noted in the text, the geometries of all species were completely optimized with no geometrical constraints using the standard BFGS method[32] and the option for increased precision (PRECISE) recommended by Stewart.[33] Transition-state geometries were first located approximately using either the reaction coordinate method[34] or contour maps; the latter were generated by fixing the forming and breaking bonds at appropriate lengths and minimizing the energy of the system with respect to all remaining variables. Approximate transition-state geometries identified in these ways were then refined using the method of McIver and Komornicki.[35] All stationary points were characterized by diagonalization of the force constant matrix; no reactant or ion–dipole complex had a negative eigenvalue, and all transition-state structures satisfied the single negative eigenvalue criterion.[36]

Results

Unimolecular Dissociation in the Gas Phase. Results for the heterolytic bond cleavage of various substrates in the gas phase are summarized in Table I. In contrast to the original MNDO method, which underestimated the heat of formation for the methyl cation by 17.4 kcal/mol,[37] the PM3 result of 256.5 kcal/mol[38] is in fairly good agreement with the experimental value of 261.3 kcal/mol[39] and was therefore chosen for this analysis. The heterolytic bond cleavage of the trimethyloxonium ion is only about half as endothermic as that for one of the nitrogen leaving groups in the tetramethylammonium cation. This reflects the different behavior of ethers and amines toward alkylation and the potential of the corresponding cations as alkylating agents. ΔH_R for the dissociation of the trimethyloxonium ion lies in the same range as the experimental value for the methyldiazonium cation.[39]

Introduction of a stabilizing methoxy substituent results in a dramatically decreased heat of reaction. In fact, bond cleavage in the case of the (methoxymethyl)dimethyloxonium cation proceeds without a barrier; the bond between the leaving dimethyl ether and the cationic intermediate had to be fixed in the calculation in order to obtain the heat of formation. The effect in the nitrogen cases is also drastic, with a decrease in ΔH_R on the order of 60 kcal/mol, but the dissociations are still endothermic.

The carbons of the ribose ring in β-nicotinamide riboside$^+$ stabilize the oxocarbenium ion intermediate by another 5 kcal/mol, with a heat of reaction for the heterolytic cleavage of the nicotinamide–ribosyl bond of 40.5 kcal/mol. The analysis of the net atomic charges shows that the developing positive charge is distributed mainly on C1′, H1′, and the ribose oxygen; the charge on C1′ increases from -0.008 to 0.352 and on H from 0.131 to 0.178, and the negative charge on the oxygen decreases from -0.242 to -0.020. While bond lengths and bond orders for the

(16) Jencks, W. P. *Chem. Soc. Rev.* **1981**, *10*, 345-375.
(17) Hwang, J. K.; King, G.; Creighton, S.; Warshel, A. *J. Am. Chem. Soc.* **1988**, *110*, 5297-5311.
(18) Harcourt, R. D. *J. Mol. Struct. (THEOCHEM)* **1988**, *165*, 329-340.
(19) Chandrasekhar, J.; Smith, S. F.; Jorgensen, W. L. *J. Am. Chem. Soc.* **1985**, *107*, 154-163.
(20) Bash, P. A.; Field, M. J.; Karplus, M. *J. Am. Chem. Soc.* **1987**, *109*, 8092-8094.
(21) Kollman, P. A.; Singh, U. C. *J. Comput. Chem.* **1986**, *7*, 718-730.
(22) Bergsma, J. P.; Gertner, B. J.; Wilson, K. R.; Hynes, J. T.; Lee, S. *J. Chem. Phys.* **1987**, *86*, 1356-1386.
(23) Kozazki, T.; Morihashi, K.; Kikuchi, O. *J. Am. Chem. Soc.* **1989**, *111*, 1547-1552.
(24) Tucker, S.; Truhlar, D. G. *J. Am. Chem. Soc.* **1990**, *112*, 3338-3361.
(25) Ford, G. P.; Scribner, J. D. *J. Am. Chem. Soc.* **1983**, *105*, 349-354.
(26) Ford, G. P. *J. Am. Chem. Soc.* **1986**, *108*, 5104-5108.
(27) Ford, G. P.; Smith, C. T. *J. Chem. Soc., Chem. Commun.* **1987**, *4*, 44-45.
(28) Stewart, J. J. P. *J. Comput. Chem.* **1989**, *10*, 209-220.
(29) Merz, K. M., Jr.; Besler, B. H. QCPE Program No. 589, *QCPE Bull.* **1990**, *10*, 15.
(30) Dewar, M. J. S.; Zoebisch, E. G.; Healy, E. F.; Stewart, J. J. P. *J. Am. Chem. Soc.* **1985**, *107*, 3902-3909.
(31) Schröder, S.; Daggett, V.; Kollman, P. A. *J. Am. Chem. Soc.* **1991**, *113*, 8922-8925.
(32) Shanno, D. F. *J. Optim. Theory Appl.* **1985**, *46*, 87.
(33) Boyd, D. B.; Smith, D. W.; Steward, J. J. P.; Wimmer, E. *J. Comput. Chem.* **1988**, *9*, 387-398.
(34) Dewar, M. J. S.; Kirschner, S. J. *J. Am. Chem. Soc.* **1971**, *93*, 4290-4291.
(35) McIver, J. W., Jr.; Komornicki, A. *Chem. Phys. Lett.* **1971**, *10*, 303-306.
(36) Flanigan, M. C.; Komornicki, A.; McIver, J. W., Jr. In *Modern Theoretical Chemistry*; Segal, G. A., Ed.; Plenum Press: New York, 1977; Vol. 9.
(37) Dewar, M. J. S.; Thiel, W. *J. Am. Chem. Soc.* **1977**, *99*, 4907-4917.
(38) Stewart, J. *Comput.-Aided Mol. Des.* **1990**, *4*, 1-105.
(39) Foster, M. S.; Williamson, A. D.; Beauchamp, J. L. *Int. J. Mass Spectrom. Ion Phys.* **1974**, *15*, 429-436.

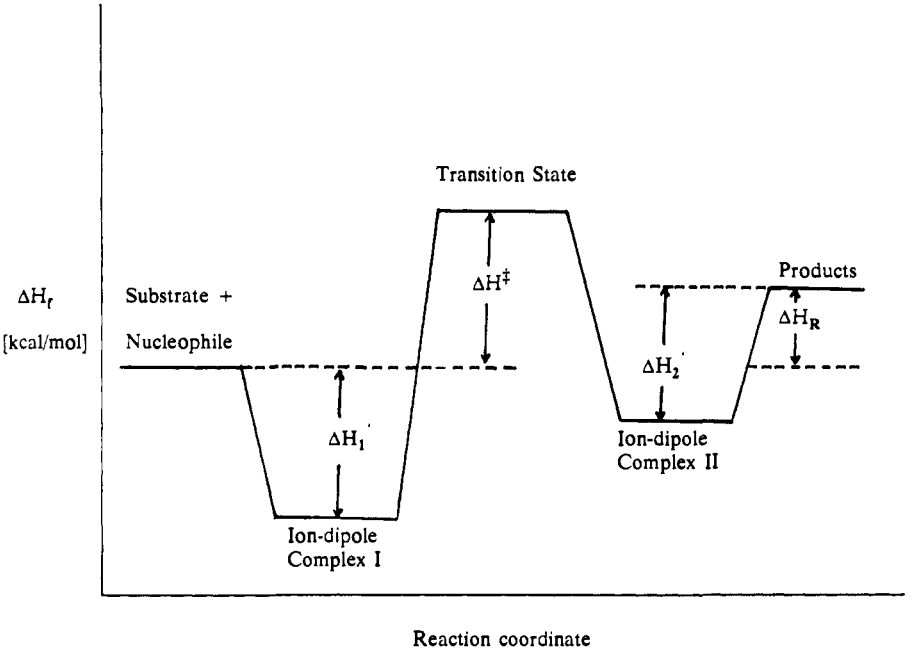

Figure 1. General profile for the isoenergetic S_N2 reactions.

C1–H1′ and C1′–C2′ bonds are changed only slightly, the bond length for the carbon–oxygen bond decreases from 1.405 to 1.270 Å, and the bond order changes from an almost pure single bond (1.012) to a bond with significant double bond character (1.634). The additional stabilization of the β-nicotinamide riboside is caused by the C2′HOH group adjacent to the carbocation. The positive charge on this group increases from 0.079 in the un-ionized species to 0.134 in the oxocarbenium ion. The length of the C1′–C2′ bond decreases from 1.566 to 1.519 Å, while the bond order increases from 0.915 to 0.939. The structure of the oxocarbenium ion intermediate thus reflects the valence bond description for a delocalized positive charge.

Gas-Phase Isoenergetic S_N2 Reactions. Results for the isoenergetic nucleophilic substitution reactions of dimethyl ether and trimethyloxonium ion, trimethylamine and tetramethylammonium ion, and chloride with β-chlororibose are summarized in Table II. We also recalculated the chloride/methyl chloride reaction with the PM3 parameter set. Comparison of the PM3 energies with previously reported calculated[19,20] and experimental[40,41] values shows that the stabilization energy $\Delta H'$ of 12.5 kcal/mol and the activation energy $\Delta H^{\ddagger} - \Delta H'$ of 13.3 kcal/mol are in excellent agreement (Table II).

All reactions follow the currently accepted reaction profile for a gas-phase, ion–molecule reaction as shown in Figure 1. In particular, the transition states are preceded by loose ion–dipole complexes with distances ranging from 2.5 and 3.0 Å between the nucleophile and the substrates. The relative orientation is exclusively dominated by the charge distribution. The binding can be considered to be entirely electrostatic, with the exception of the ribose system in which hydrogen bonding to the incoming nucleophile is observed (Figure 2) and accounts for the unusual stabilization of the ion–dipole complex.

The importance of the use of high-precision optimizations in these studies is illustrated by the comparison of two preliminary AM1 calculations on the ion–dipole complex for the trimethyloxonium ion–dimethyl ether reaction. Without the PRECISE option, which increases convergence criteria by a factor of 100, a structure closely related to the nearest point from the reaction coordinate calculation is obtained (structure **1** in Figure 3), whereas the real gas-phase ion–dipole complex for AM1 and the PM3 method resembles the highly symmetrical structure **2**. Even

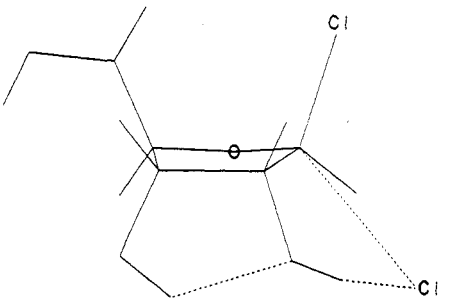

Figure 2. PM3 structure for the chloride–chlororibose ion–dipole complex.

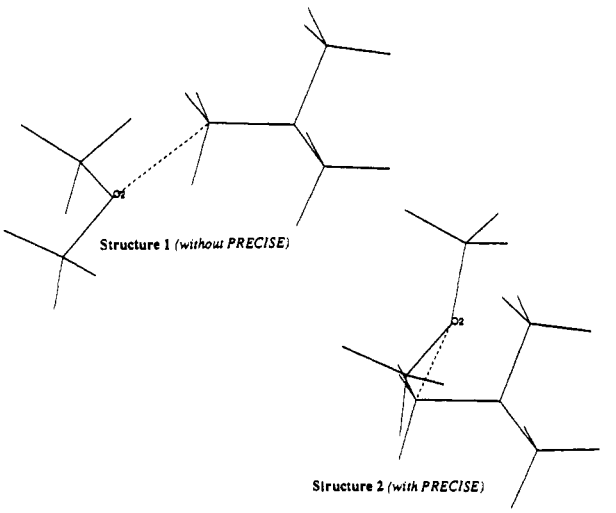

Figure 3. AM1 structures for the dimethyl ether–trimethyloxonium cation ion–dipole complex. Structure **1**, without the PRECISE option; structure **2**, with the PRECISE option.

in cases where structural deviations are smaller, the rigorously optimized structure can still lead to a decrease in the heat of formation of up to 4 kcal/mol.

The structure of the ion–dipole complex **2** led us to investigate the effect of nucleophilic assistance on the course of the reaction. As the overall energetics of reaction 2 in Table II show, no facilitation of the S_N2 process was observed when a second dimethyl

(40) Dougherty, R. C.; Roberts, J. D. *Org. Mass Spectrom.* **1974**, *8*, 77.
(41) Pellerite, M. J.; Brauman, J. I. *J. Am. Chem. Soc.* **1983**, *105*, 2672–2680.

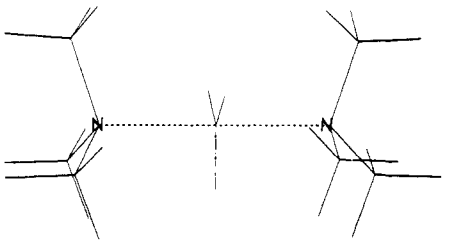

Figure 4. PM3 transition-state structure for the trimethylammonium–tetramethylammonium cation reaction.

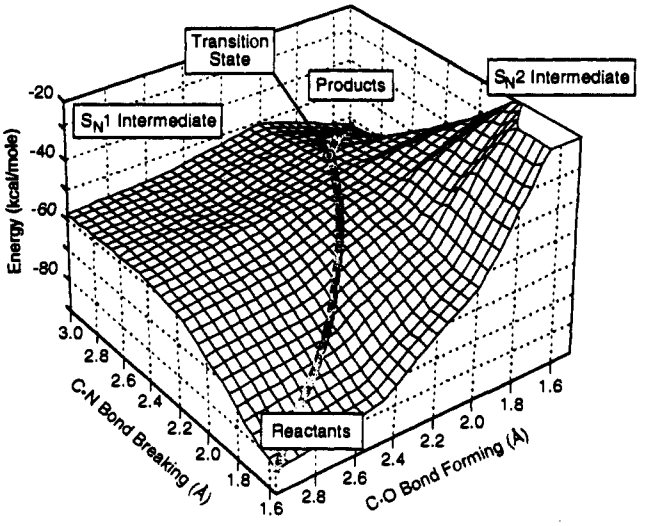

Figure 5. Contour drawing of the dissociation energies for the inversion reaction of β-nicotinamide riboside with water taken from Table III. The drawing was made using the S-language package from AT&T; the energies were interpolated onto a 30 × 30 grid with an arbitrary cutoff of energies higher than −20 kcal/mol.

ether molecule approached the ion–dipole structure **2**.

The calculated transition-state geometries correspond to the established representation of the S_N2 transition state in which the entering group, leaving group, and inverting carbon atom are approximately collinear. The transition-state structure for the reaction of trimethylamine with the tetramethylammonium cation is given in Figure 4 as a representative example.

Gas-Phase S_N2(type IV) Reaction of β-Nicotinamide Riboside$^+$ and Water. The investigation of β-nicotinamide riboside$^+$ hydrolysis was begun by calculating the PM3 potential energy surface for the reaction with inversion of the C1′ carbon center using a grid search technique. The two reacting bonds were fixed at given distances while the rest of the molecule was fully optimized. The potential surface was obtained by varying the breaking N–C1′ bond in steps of 0.2 Å and the forming C1′–O bond in steps of 0.5 Å. The results are summarized in Table III and shown graphically in Figure 5. Optimization starting from the structures in the upper left (reactant side of the surface, grid point 1.52 Å/3.0 Å) and lower right corners (product side, grid point 2.9 Å/1.5 Å) of Table III without any geometrical constraints resulted in the ion–dipole complexes for water interacting with β-nicotinamide riboside$^+$ and nicotinamide hydrogen bonded to the α-hydrated ribose cation, respectively. The pseudo minimum energy pathway connecting these two states proceeds first to structures in which the N–C1′ bond is almost entirely broken before the approach of water becomes more favored energetically. The grid point at 2.9 Å/2.0 Å was therefore chosen as the starting point for a successful transition-state optimization that led to the structure shown in Figure 6.

A similar approach for the water attack on β-nicotinamide riboside$^+$ with retention of the carbon center showed that, as long as the N–C1′ bond is not significantly lengthened, the water will prefer to attack the back side because of the stabilization gained from the hydrogen bonding of the incoming nucleophile to the

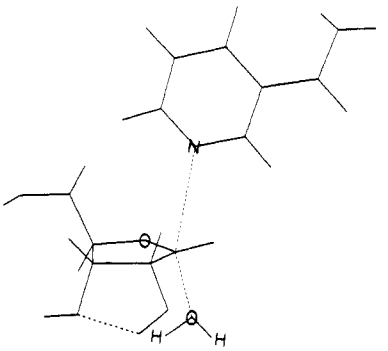

Figure 6. PM3 transition-state structure for the β-nicotinamide riboside hydrolysis with inversion.

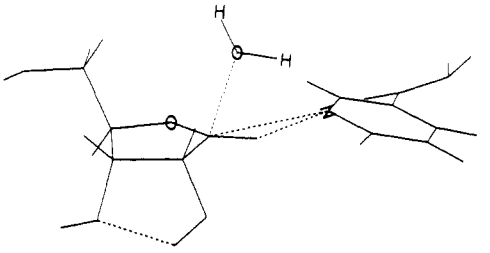

Figure 7. PM3 transition-state structure for the β-nicotinamide riboside hydrolysis with retention.

2′-hydroxyl group of the sugar. But once the N–C1′ bond is increased to about 2.9 Å, retention is slightly favored and the calculated transition state (Figure 7) is 1.2 kcal/mol lower in energy than the one for the inversion path. The extreme stabilization of the retention type ion–dipole complex of nicotinamide and the α-hydrated ribose cation is the result of the hydrogen bonding of the leaving group to one of the water hydrogens, and thus it resembles a preformed proton-transfer structure with an extended oxygen–hydrogen bond of 1.03 Å. The results are summarized in the energy profile shown in Figure 8.

Discussion

Extrapolation of the calculated results for the isolated reactants in the gas phase to their behavior in solution entails several uncertainties. Nevertheless, a detailed understanding of the fundamental determinants, especially the heights of the activation barriers, should provide a valuable framework for a discussion of the solution-phase results. The relative $\Delta H^{\ddagger}$ values can be rationalized in terms of a superposition of electrostatic and covalent interactions.[42] Comparison of the overall activation barriers for the reactions considered here shows that the calculated $\Delta H^{\ddagger}$ values increase from the two processes with chloride as the nucleophile to the trimethyloxonium case and the β-nicotinamide riboside$^+$ hydrolysis and to the displacement of trimethylamine in the tetramethylammonium cation. The form of the potential energy profiles (Figures 1 and 8) provides a convenient qualitative separation of this kind. The depths of the wells in which the ion–dipole complexes reside should give an approximate indication of the magnitude of the electrostatic stabilization of the activated complexes. Stabilization of covalent interactions should then be reflected in the heights of the central barrier above the corresponding complexes.[25]

The smaller $\Delta H^{\ddagger} - \Delta H'$ barriers in the S_N2(type I) reactions with chloride can be attributed to its much lower ionization potential of 3.5 eV (compared to 10.7 eV for dimethyl ether) and the favorable HOMO–LUMO interaction in this case. This is generally accepted as the initial step of a nucleophile displacement[43] and is related to the availability of the nucleophile electrons for bond formation during the course of the reaction. The sur-

(42) Klopman, G. In *Chemical Reactivity and Reaction Paths*; Klopman, G., Ed.; Wiley-Interscience: New York, 1974; pp 55–165.
(43) Fukui, K. *Angew. Chem., Int. Ed. Engl.* **1982**, *21*, 801–809.

Table II. Calculated Energies for the S_N2 Reactions[a]

reaction	nucleophile	ΔH_f	substrate	ΔH_f	ΔH_f(ID1)	ΔH_f(TS)	H_f(ID2)	$\Delta H_1'$[b]	$\Delta H^{\ddagger}$[c]	$\Delta H^{\ddagger} - \Delta H_1'$	$\Delta H_2'$[d]	ΔH_R	comment
1	$(CH_3)_2O$	−48.3	$(CH_3)_3O^+$	161.0	104.9	129.0		−7.8	16.3	24.1		0	isoenergetic
2	$2X\ (CH_3)_2O$	−96.6	$(CH_3)_3O^+$	161.0	47.9	71.7		−16.5	7.3	23.8		0	isoenergetic
3	$(CH_3)_3N$	−10.9	$(CH_3)_4N^+$	149.4	128.9	170.5		−9.6	32.0	41.6		0	isoenergetic
4	Cl^-	−52.2	CH_3Cl	−14.7	−78.4	−65.1		−12.5	0.8	13.3[e]		0	isoenergetic
5	Cl^-	−52.2	β-chlororibose	−184.9	−269.9	−248.4	−251.1	−33.8	−12.3	21.5	−16.7	1.7	α-chlororibose, ΔH_f = 182.2
6	H_2O	−53.4	β-nicotinamide riboside	−23.3	−85.2	−50.5	−63.2	−8.5	26.2	34.7	−12.6	26.1	ribose–water$^+$ inversion, ΔH_f = −41.8[f]
7	H_2O	−53.4	β-nicotinamide riboside	−23.3		−51.8	−68.2		24.9	33.4[g]	−25.7	34.2	ribose–water$^+$ retention, ΔH_f = −33.7

[a] Energies are in kcal/mol. [b] Stabilization of the ion–dipole complex 1: $\Delta H_1' = \Delta H_f(\text{ID1}) - [\Delta H_f(\text{nucleophile}) - \Delta H_f(\text{substrate})]$. [c] Activation barrier relative to reactants: $\Delta H^{\ddagger} = \Delta H_f(\text{TS}) - [\Delta H_f(\text{nucleophile}) - \Delta H_f(\text{substrate})]$. [d] Stabilization of the ion–dipole complex 2: $\Delta H_2' = \Delta H_f(\text{ID2}) - \sum \Delta H_f(\text{products})$. [e] For comparison: MNDO, $\Delta H_1' = -7.3$, $\Delta H^{\ddagger} - \Delta H_1' = 10.5$ (ref 18); AM1, $\Delta H_1' = -8.6$, $\Delta H^{\ddagger} - \Delta H_1' = 9.1$ (ref 18); 6-31G*, $\Delta H_1' = -10.3$, $\Delta H^{\ddagger} - \Delta H_1' = 13.9$ (ref 17); exptl, $\Delta H_1' = -8.5$ (ref 38), $\Delta H^{\ddagger} - \Delta H_1' = 10$–14 (ref 39). [f] ΔH_f(nicotinamide) = −8.8 kcal/mol (see Table I). [g] Value relative to ID1 (inversion).

prisingly low value of $\Delta H^{\ddagger}$ for the reaction of chloride with β-chlororibose is dominated by the electrostatic stabilization in the ion-pair complex because the $\Delta H^{\ddagger} - \Delta H'$ barrier is significantly higher than that for the methyl chloride reaction. This increase can be attributed to steric hindrance and a less favorable HOMO–LUMO interaction in the sugar. In contrast, S_N2(type IV) reactions are characterized by nucleophiles with considerably less available electron density (ionization potentials in the range 9.1–12.3 eV) and less favorable HOMO–LUMO interactions (compared with the oxonium model). The generally higher $\Delta H^{\ddagger} - \Delta H'$ barriers can thus be explained by the smaller contribution of covalent stabilization in the transition state.

The bond lengths and bond orders around the reaction center and the frequencies of the imaginary vibrations (calculated from the appropriate eigenvector of the force constant matrix[36]) for all activated complexes are summarized in Table IV. These properties provide a measurement of the "looseness" of a transition state; in the series considered here, trimethylamine with tetramethylammonium cation is the "tightest" followed by the trimethyloxonium ion and methyl chloride reactions. The three reactions involving the ribose system are considerably more "open", however. This behavior can be interpreted with the arguments made by Ford and Scribner in their discussion of the reactivity of diazonium ions.[25] The differences in the transition-state geometries for the S_N2 processes can be related directly to the thermodynamics of the corresponding unimolecular dissociations. Formation of the methyl cation in the case of the tetramethylammonium cation is by far the most endothermic process that forces the activated complex to be extremely tight and, because of steric crowding, highly energetic. The activated complex for the oxonium reaction is considerably more open, which reflects the significantly more facile heterolytic bond cleavage. The systems involving the sugar moiety exhibit extremely low bond orders and vibrational frequencies. Note the fact that the bond to the incoming nucleophile is short because of hydrogen bonding with the 2′-hydroxyl group discussed above.

The relation of the transition-state geometries to the heat of reaction for heterolytic bond cleavage gives a more precise meaning to the concept of the "S_N1 character" of a formally bimolecular reaction. That it is a two-dimensional application of the Hammond postulate[44] can be shown using the potential energy surface for the β-nicotinamide riboside$^+$ hydrolysis (Figure 5, data from Table III). As the S_N1 intermediate becomes more stabilized, the energy in the upper left region of the plot decreases, which favors the displacement of the pseudo minimum energy path including the transition state in this direction. Because the oxocarbenium ion intermediate is strongly stabilized by the introduction of the sugar moiety with respect to methyl cation, the transition-state structure "loosens" and the "S_N1 character" of the reaction increases. This phenomenon can be seen in the α-chlororibose reaction with a frequency of 346 cm^{-1} compared to 510 cm^{-1} for the methyl chloride case.

For the type IV nucleophilic substitution reaction of β-nicotinamide riboside$^+$ with the poor nucleophile water (ionization potential of 12.3 eV), the bond distance to the leaving group is 3.011 for inversion and 2.884 Å for retention, with bond orders of 0.002 and 0.036, respectively. These values are in good agreement with estimates from the measurement of kinetic α-secondary deuterium isotope effects.[10,11] The activated complex for retention is slightly tighter, with a frequency of 200 cm^{-1} compared to 154 cm^{-1} for inversion, whereas the bond to the incoming nucleophile is a bit shorter in the latter instance. Because of π-character, the C1′–O bond has a distance of 1.294 Å and a bond order of 1.458 for inversion and values of 1.289 Å and 1.482 Å for retention, which is almost as developed as in the free oxocarbenium ion (1.270 Å, 1.634 Å).

The structure for the inversion reaction closely resembles the "exploded" transition state for the solvolysis of D-glucopyranosyl derivatives suggested by Sinnott and Jencks.[15] The anomeric center in the activated complex has a significant amount of sp^2

(44) Hammond, G. S. *J. Am. Chem. Soc.* **1955**, *77*, 334–338.

Table III. Grid Search for the Inversion Attack of Water on β-Nicotinamide Riboside+ [a]

$r_{(C-O)}$ bond forming	$r_{(N-C)}$ bond breaking[b] 1.52	1.70	1.90	2.10	2.30	2.50	2.70	2.90
3.00	−84.9	−79.6	−69.2	−60.8	−57.2	−56.7	−57.1	−57.2
2.50	−79.4	−74.8	−65.2	−57.0	−52.9	−54.9	−55.2	−55.2
2.00	−54.0	−53.5	−49.0	−46.1	−46.3	−47.9	−49.5	−50.2
1.50	+10.7	−5.3	−19.5	−32.7	−43.4	−54.5	−61.2	−62.2

[a] ΔH_f values are in kcal/mol. [b] Bond distances are in Å.

Table IV. Charge Analysis for β-Nicotinamide Riboside Inversion and Retention Reactions

	$\Sigma_{nicotinamide}$	Σ_{sugar}	Σ_{water}	C_1'	H_1'	O	$N_{nicotinamide}$	$\Sigma_{C2'OH}$
inversion								
reactants	0.805	0.195	0	−0.007	0.131	−0.242	0.437	0.079
ID1	0.798	0.174	0.028	−0.065	0.191	−0.239	0.454	0.070
TS	0.006	0.871	0.123	0.391	0.173	−0.073	−0.198	0.098
ID2	0.100	0.372	0.528	0.066	0.246	−0.263	−0.118	0.061
products	0	0.473	0.527	0.193	0.159	−0.256	−0.083	0.082
retention[a]								
TS	0.096	0.844	0.060	0.303	0.226	−0.073	−0.187	0.101
ID2	0.194	0.393	0.413	0.186	0.131	−0.267	−0.102	0.086
products	0	0.520	0.480	0.201	0.169	−0.234	−0.083	0.092
S_N1 intermediate (oxocarbenium ion)				0.352	0.177	−0.020		0.134

[a] An ion–dipole complex of substrate and nucleophile (reactants) was not observed (see text).

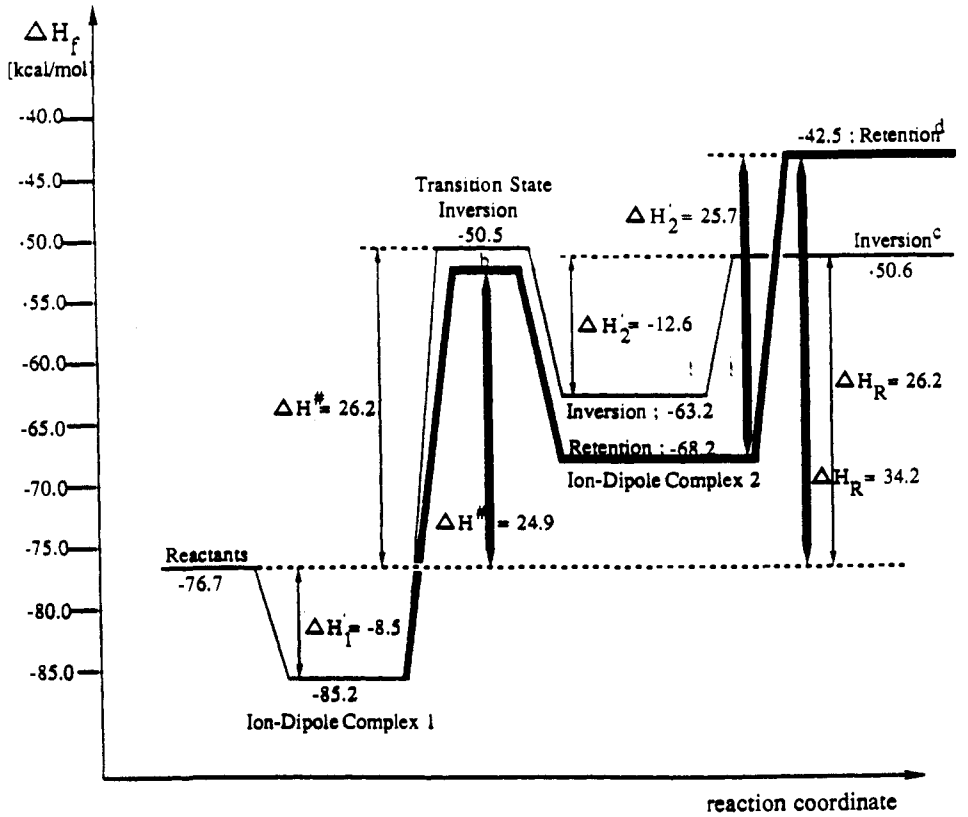

(a) $\Delta H_f(H_2O)$ = -53.4 ; ΔH_f (β-nicotinamide-riboside) = -23.3

(b) Transition State Retention ; -51.8

(c) ΔH_f(Ribose-water$^-$) = -41.8 ; ΔH_f(Nicotinamide) = -8.8

(d) ΔH_f(Ribose-water$^-$) = -33.7 ; ΔH_f(Nicotinamide) = -8.8

Figure 8. Calculated reaction profile for the bimolecular hydrolysis of β-nicotinamide riboside.

hybridization and a high degree of charge separation, but the still visible bond orders between the anomeric carbon and the leaving group as well as the incoming nucleophile indicate that the interaction at the transition state is not entirely electrostatic and can account for the experimental evidence of nucleophilic participation.[15]

An analysis of the charges in the two species clarifies this point. The sugar moiety has a charge of 0.871/0.844 in the transition states compared with the S_N1 intermediate. Water has most of the remaining charge of 0.123 in the inversion reaction—the sugar–nicotinamide bond is extremely long, 3.011 Å, and little interaction with the nitrogen is possible. Charge is more evenly

distributed in the activated complex for the retention reaction because of a shorter bond length to the leaving group and because of possible interactions between water and nicotinamide on the same face of the sugar. With the exception of ion–dipole complex II for the retention reaction, which resembles a preformed proton-transfer structure, ion–dipole complexes do not show a great deal of charge transfer. In both cases, the reaction center has a partial charge of the same order (0.391 and 0.303, respectively) as the oxocarbenium ion (0.352). The absolute value seems to be affected strongly by the looseness of the transition state (compare Table IV).

Thus, charge migrates from nicotinamide to the sugar and, in the transition state, to the incoming water molecule. From their computational study of solvent effects in the Menshutkin reaction, Bertrán and his colleagues[45] noted that effects on the activation barrier depend on differential solvation of the ground and transition states. In contrast to the type I reaction of chloride with methyl chloride in which a single atom with unit charge is highly solvated, charge in our system is delocalized. Only a slight increase in the activation barrier would be expected in solution, but because of the uncertainties inherent in comparing gas- and solution-phase reactions, this conclusion is certainly tentative.

Sinnott and Jencks seem to have pictured the exploded transition state as a *single* entity that partitions between retained and inverted products (Structure III of ref 15). Our calculated structures for the activated complexes for the inversion and retention reactions have quite different angles between the leaving group nitrogen and the anomeric carbon (Figures 6 and 7, respectively) and have slightly different energies that favor retained over inverted products. Sinnott and Jencks note that "[i]f it were not for the formation of products with retention of configuration...there would be no sharp line separating this kind of interaction from that in the classical S_N2 displacement reaction.... [W]hen a transition state is sufficiently open...these interactions can be significantly on the same as well as on the opposite side of the central atom as the leaving group" (ref 15, p 2032). The flatness of the plane in the contour diagram (Figure 5) on which the transition state for the *inversion* reaction lies shows that, even with a well-defined back-side LUMO–HOMO interaction, the activated complex is open. The structure of the activated complex for the retention reaction (Figure 7) is quite different from the retention channel of the exploded transition state in drawing III of Sinnott and Jencks.[15] We interpret this difference to be the result of noncovalent interactions between water and the leaving group in the retention reaction. Both of the calculated activated complexes have the specific but weak interactions between the anomeric carbon and both the leaving group and incoming solvent suggested by Sinnott and Jencks.[15]

The gas-phase dissociation of a series of 2′-substituted β-nicotinamide arabinosides[9] has been measured using tandem liquid secondary ion mass spectrometry (LSIMS).[46] Dissociation of the sorted molecular ion for five substrates follows the Taft LFER ($\rho_I = -0.89$, $r = 0.95$), and the log of the relative rates in the gas phase correlate quite well with the log of the first-order rate constants for the pH-independent hydrolysis reaction ($r = 0.96$).[47] Thus, the relative order and stabilities of the oxocarbenium ion intermediates are the same in either phase. There is evidence from a rearrangement channel for the 2′-HNAc substrate that an ion–dipole complex is formed as an intermediate in dissociation; by the Hammond postulate,[44] a late transition state is product like, which in this instance is the ion–dipole complex and is consistent with the computationally derived extent of bond breaking at the transition state.

Conclusions. The type IV nucleophilic substitution reactions investigated here follow the same overall energy profile that is expected for a gas-phase ion–molecule process. In particular, the transition states are preceded by an ion–dipole complex with entirely electrostatic interaction. The reactions involving a neutral nucleophile and a positively charged substrate generally require a higher activation energy, which can be attributed to the poorer nucleophilicity and to a less favorable HOMO–LUMO interaction compared to the S_N2(type I) processes. The increasing S_N1 character for a bimolecular reaction can be directly related to the stabilization of the corresponding unimolecular dissociation. This phenomenon explains the extremely "loose" transition states for the inversion and retention attack of water on β-nicotinamide riboside$^+$ in the gas phase and offers a satisfying rationalization of the experimental data for the β-nicotinamide riboside$^+$ hydrolysis in solution. Given the general importance of type IV nucleophilic substitution reactions, not only for the cleavage of an N–glycosyl bond in β-nicotinamide riboside$^+$ but also for a number of related chemical and enzymatic reactions,[48] the ideas presented in this paper should facilitate our understanding of the mechanisms of nucleophilic substitution.

Acknowledgment. We are pleased to acknowledge the support of the NIH (GM-29072, to P.A.K., and GM-22982, to N.J.O.), the Deutsche Forschungsgemeinschaft for a postdoctoral fellowship (S.S.), and funds from a State of California Biotechnology Grant (N.B.). The authors acknowledge the use of the facilities of the UCSF Computer Graphics Laboratory, R. Langridge, principal investigator, which are supported by NIH Grant RR-1081. We thank John M. Troyer for the contour drawing (Figure 5).

Supplementary Material Available: Tables of calculated Cartesian coordinates for all species optimized in this report (25 pages). Ordering information is given on any current masthead page.

(45) Solà, M.; Lledós, A.; Duran, M.; Bertrán, J.; Abboud, J.-L. M. *J. Am. Chem. Soc.* **1991**, *113*, 2873–2879.

(46) Buckley, N.; Handlon, A. L.; Maltby, D.; Burlingame, A. L.; Oppenheimer, N. J. Submitted for publication.

(47) The yields from dissociation are relatively high. For example, for the 2′-H-substituted oxocarbenium ion, the most stable of the ions, the ratio of M^+ to total oxocarbenium ion related cations is 1:0.33.

(48) Parkin, D. W.; Schramm, V. L. *J. Biol. Chem.* **1984**, *259*, 9418–9425.